Proceedings of the Combustion Institute, Volume 28, 2000/pp. 41–49

SCALAR MIXING AND DISSIPATION RATE IN LARGE-EDDY SIMULATIONS OF NON-PREMIXED TURBULENT COMBUSTION

HEINZ PITSCH AND HELFRIED STEINER
Center for Turbulence Research
Flow Physics and Computation Division
Stanford University
Stanford, CA 94305-3030, USA

Predictions of scalar mixing and the scalar dissipation rate from large-eddy simulations of a piloted non-premixed methane/air diffusion flame (Sandia flame D) using the Lagrangian-type flamelet model are presented. The results obtained for the unconditionally filtered scalar dissipation rate are qualitatively compared with general observations of scalar mixing from experiments in non-reactive and reactive jets. In agreement with experimental data, provided the reaction zone has an inward direction, regions of high scalar dissipation rate are organized in layerlike structures, inwardly inclined to the mean flow and aligned with the instantaneous reaction zone. The analysis of single-point time records of the mixture fraction reveals ramplike structures, which have also been observed experimentally and are believed to indicate large-scale turbulent structures. The probability density function (pdf) of the instantaneous resolved scalar dissipation rate at stoichiometric mixture evaluated at cross sections normal to the the nozzle axis is shown to be described accurately by a lognormal pdf with $\sigma = 1$. A new model for the conditionally averaged scalar dissipation rate has been proposed and is shown to account for local deviations from the simple mixing layer structure. The stabilizing effect of the pilot flame in the present configuration is also discussed. Finally, the influence of the resolved fluctuations of the scalar dissipation rate on the flame structure is investigated, revealing only a weak influence on temperature and nitric oxide predictions. However, the model requires further refinement for situations in which local extinction events become important.

Introduction

The mixing of scalars in turbulent flows is a very interesting problem which provides a fundamental understanding of the basic processes involved in non-premixed combustion problems and has been investigated by many in this field. A comprehensive review of experimental findings has recently been provided by Pitts et al. [1].

In non-premixed combustion, chemical reactions occur only if fuel and oxidizer are mixed at the molecular level. Although turbulent mixing is responsible for stirring the reactants at large scales, it contributes to the molecular scalar mixing only indirectly, increasing the scalar variances and thereby the scalar gradients. Molecular mixing essentially occurs at the smallest turbulent scales by removal of the scalar variance. The rate of molecular scalar mixing is represented by the scalar dissipation rate, which can be identified as the most important parameter in the description of non-premixed combustion.

Because combustion can occur only if the reactants are mixed on the molecular level, the scalar dissipation rate provides a measure of the maximum possible chemical reaction rate. This is the basic idea of the eddy break-up model [2]. Assuming infinitely fast chemistry, it has been shown by Bilger [3] that the turbulent reaction rate is linearly proportional to the scalar dissipation rate at stoichiometric conditions, χ_{st}. For finite-rate chemistry, the scalar dissipation rate appears as a parameter in most of the commonly applied combustion models such as the flamelet model [4,5], the transported probability density function model [6,7], and the conditional moment closure model [8].

The influence of the scalar dissipation rate, χ, on the structure of diffusion flames has been discussed by Peters [4]. In general, the scalar dissipation rate at the stoichiometric mixture fraction describes the departure from chemical equilibrium. If the stoichiometric scalar dissipation rate in a steady laminar diffusion flame exceeds a critical value, χ_q, the flame will be quenched. However, it has been found in experiments [9,10] and numerical simulations [11–13] that the flame structure cannot instantaneously follow changes in χ_{st} and that in the case of a fluctuating scalar dissipation rate, instantaneous values of χ_{st} can by far exceed χ_q without quenching the flame. On the other hand, it is possible for the mean scalar dissipation rate to be smaller than χ_q and yet the flame may be quenched by fluctuations above this limit. In situations where local quenching occurs, it might therefore be of great importance to

accurately model the fluctuations of the scalar dissipation rate.

For the modeling of the scalar dissipation rate, large-eddy simulations have the advantage of resolving the major part of the turbulent motion. Only the fluctuations which occur on smaller length scales than the filter width, typically given by the spacing of the numerical discretization, have to be modeled. The modeling effort of the basic quantities such as subgrid scale stresses and variances is supported by the concept of a turbulent energy cascade in two different ways. First, most of the turbulent energy is in the resolved scales. Second, the energy cascade concept suggests that subgrid quantities can be universally related to the resolved field. In contrast, since the dissipation of scalar variance occurs essentially at the smallest scales, the major part of the scalar dissipation rate has to be modeled. Following the energy cascade concept, the scalar dissipation rate is, similar to the turbulent kinetic energy dissipation rate, a universal quantity describing the scalar variance transport in wavenumber space, and knowledge of the resolved-scale field should hence be beneficial in the determination of the scalar dissipation rate as a fluctuating quantity.

In this paper, we describe and evaluate the modeling of the scalar dissipation rate and its fluctuations in large-eddy simulations (LES) for non-premixed combustion using the Lagrangian-type flamelet model [14,15]. The predictions of the unconditional mean scalar dissipation rate from an LES of a piloted turbulent diffusion flame (Sandia flame D [16,17]) is discussed and compared to general and mainly qualitative observations from several experiments. The influence of resolved fluctuations of the modeled conditional scalar dissipation rate on the chemical flame structure is investigated by comparing the results of calculations, which include the fluctuations of the scalar dissipation rate, with results for the same configuration obtained by using time-averaged values for the scalar dissipation [18].

We first give a brief review of the Lagrangian-type flamelet model as a combustion model for LES and present a new model for the evaluation of the conditional mean scalar dissipation rate. We then discuss the results for the unconditional resolved scalar dissipation rate, and finally the influence of the resolved fluctuations of the conditional mean scalar dissipation rate.

Model Formulation

Large-Eddy Simulation

The system of equations to be solved is given by the spatially filtered continuity, momentum, and mixture fraction equations provided, for instance, by Moin et al. [19]. The subgrid stresses and the velocity-mixture fraction covariance appearing in the momentum equations and in the mixture fraction equation are expressed by eddy-viscosity-type models, where the eddy viscosity is given by the Smagorinsky model, the eddy diffusivity, D_t, by the assumption of a constant turbulent Schmidt number, $Sc_t = 0.4$ [18]. Following Pierce and Moin [19], the mixture fraction variance is given by

$$\widetilde{Z''^2} = C_Z \Delta^2 (\nabla \tilde{Z})^2 \tag{1}$$

The Smagorinsky coefficient and the coefficient C_Z are computed from the solution of the resolved scales by applying the dynamic procedure [20]. No model constants have to be specified in the computation of the flow field. The simulation was performed in a spherical coordinate system with 192 cells in the downstream direction, 110 cells in the cross-flow direction, and 48 cells in the azimuthal direction. The inflow conditions were prescribed according to the experimental conditions. Detailed information on the numerical procedure has been given in Ref. [18].

Lagrangian-Type Flamelet Model

In the present simulations, the Lagrangian-type flamelet model was employed to describe turbulence/chemistry interactions. The model was developed in the framework of Reynolds averaged simulations [14,15] and was recently applied in LES [18]. The model follows the conserved scalar approach, implying that the temperature and the species mass fraction can be related to the mixture fraction. Thus, density-weighted filtered quantities are given by

$$\tilde{\phi} = \int_0^1 \phi(Z)\tilde{P}(Z)dZ \tag{2}$$

where ϕ stands for the temperature, T, and the species mass fractions, Y_i. $\tilde{P}(Z)$ is the subgrid scale Favre probability density function (pdf) of the mixture fraction, Z, which is presumed to be a β-function, whose shape is determined by the resolved mixture fraction and its subgrid scale variance. The function Y_i is given by the solution of the unsteady flamelet equations. For the species mass fractions, for example, these are given as

$$\frac{\partial Y_i}{\partial \tau} - \rho \frac{\chi}{2} \frac{\partial^2 Y_i}{\partial Z^2} - \dot{m}_i = 0 \tag{3}$$

Here, τ is the Lagrangian flamelet time, ρ is the density, $\dot{m}_i$ is the chemical production rate per unit volume, and following Ref. [14], χ is given by the conditional scalar dissipation rate $\langle \chi | Z \rangle$ (τ). Lewis numbers of the chemical species have been assumed to be unity. Lagrangian flamelet particles are assumed to be introduced at the nozzle exit and travel downstream essentially with the axial velocity at stoichiometric mixture fraction. Then, τ can be related

to the physical space coordinate in the axial direction x as

$$\tau = \int_0^x \frac{1}{\langle \tilde{u}_{\tilde{Z}} | \tilde{Z}_{st} \rangle (x', t)} dx' \quad (4)$$

where $\langle \tilde{u}_{\tilde{Z}} | \tilde{Z}_{st} \rangle$ denotes the velocity of the stoichiometric mixture fraction surface in the axial direction. The resolved mass fractions can then be determined as a function of time and space with equations 2, 3, and 4, provided the conditional scalar dissipation rate is given as a function of the flamelet time, τ, and the mixture fraction, Z.

Scalar Dissipation Rate

The unconditionally filtered scalar dissipation rate is expressed in terms of the eddy diffusivity and the gradient of the resolved mixture fraction using the first-order model given by Girimaji and Zhou [21] as

$$\tilde{\chi} = 2(D_Z + D_t) (\nabla \tilde{Z})^2 \quad (5)$$

where D_Z is the molecular diffusivity of the mixture fraction.

As pointed out earlier, the temporal development of the scalar dissipation rate appearing in equation 3 is unknown and has to be related to the unconditional mean given by equation 5. A common approach to achieve this is to presume the functional dependence of the scalar dissipation rate on the mixture fraction as $\langle \chi | Z \rangle = \langle \chi_{st} \rangle f(Z)$, using analytic expressions for the function $f(Z)$ as suggested in the literature [4,14,22]. Then, it is sufficient to determine the value conditioned on stoichiometric mixture. $\langle \chi_{st} \rangle$ can then be determined by introducing the expression for $\langle \chi | Z \rangle$ in the equation for the filtered scalar dissipation rate, $\tilde{\chi}$, which can be written as

$$\tilde{\chi}(\mathbf{x}, t) = \int_{Z=0}^{1} \langle \chi | Z \rangle (x, t) \tilde{P}(Z, \mathbf{x}, t) dZ \quad (6)$$

It is demonstrated below that the function $f(Z)$ cannot be represented by the commonly applied expressions for unsteady mixing layers or counterflow diffusion flames, since in the present study a piloted flame is considered.

Here, a new model for the computation of the conditional average of the scalar dissipation rate, which has to be specified as a function of the axial distance from the nozzle as $\langle \chi | Z \rangle (x, t)$, is proposed. This model is similar to the approach used by Bushe and Steiner [23] for the estimation of chemical source terms. The term $\langle \chi | Z \rangle (x, t)$ is computed by the inversion of the integral in equation 6. Writing equation 6 for each computational cell in a chosen plane normal to the nozzle axis gives

$$\tilde{\chi}_i(x, t) = \int_{Z=0}^{1} \langle \chi | Z \rangle (x, t) \tilde{P}_i(Z, x, t) dZ,$$

$$i = 1, \ldots, N_c(x) \quad (7)$$

Here, $N_c(x)$ is the number of cells in the plane considered. If the continuous function $\langle \chi | Z \rangle (Z, x, t)$ in equation 7 is approximated by a discrete representation in terms of the mixture fraction as $\langle \chi | Z_j \rangle (x, t)$, $j = 1, \ldots, N_Z$, where N_Z *denotes the number of values used to represent the mixture fraction space, the integral in equation 7 can be approximated by a sum using, for example, the trapezoidal integration rule as*

$$\tilde{\chi}_i(x, t) \approx \sum_{j=1}^{N_Z} A_{ij} \langle \chi | Z \rangle (Z_j, x, t),$$

$$j = 1, \ldots, N_Z \quad (8)$$

where the coefficient matrix A_{ij} contains the discretized pdf $\tilde{P}_i(Z_j, x, t)$ and the coefficients of the numerical integration scheme.

Equation 8 represents a system of $N_c(x)$ equations for N_Z unknowns. For $N_c(x) > N_Z$, this can be solved by minimizing the resulting error of the overdetermined system via a least squares approach.

An alternative method to compute the conditional scalar dissipation rate has been proposed by Janicka and Peters [24]. In the transport equation of the mixture fraction pdf [7], the conditional scalar dissipation rate appears in the term representing molecular mixing. If the mixture fraction pdf is prescribed, this equation can be used to determine $\langle \chi | Z \rangle$. The underlying assumptions of this approach, which include the use of modeled values of the unconditional mean and assumed β-function shape of the mixture fraction pdf, are very similar to the model presented here. In contrast to this, the pdf transport equation method in principle provides averages over one computational cell, while the method proposed in this work is an average over a larger number of cells. However, for small values of the mixture fraction pdf, the determination of the conditional scalar dissipation rate from the pdf transport equation becomes singular, which makes its application difficult, particularly in LES, where the subgrid pdf is nonzero only in a very narrow range around the mean.

Results and Discussion

In this section, the predicted results for scalar mixing and the scalar dissipation rate from an LES of a piloted non-premixed methane/air diffusion flame (Sandia flame D) with a Reynolds number of $Re = 22000$ are presented and discussed. The instantaneous conditional scalar dissipation rates, which are obtained in the LES from equation 8, have been averaged in time and then used in the solution of the flamelet equations. This assumption is discussed below.

Experimental data for axial velocity and root mean square (RMS) has been determined by Hassel [25], while data for the mean and RMS of the temperature, and mean and conditional mean mass fractions of the chemical species CH_4, O_2, H_2, H_2O, CO,

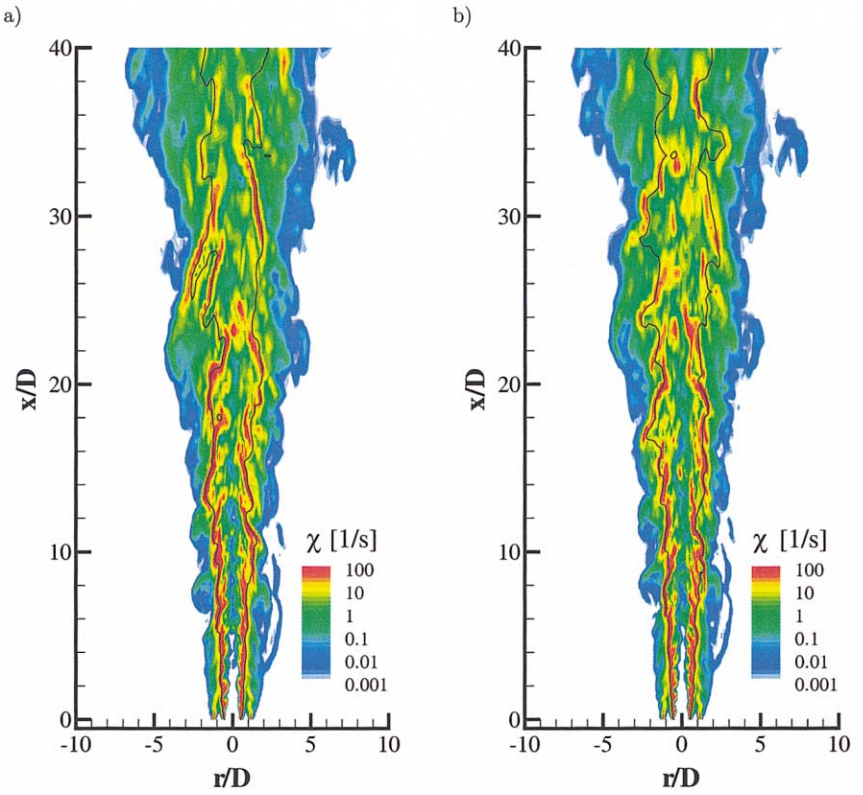

FIG. 1. Resolved instantaneous scalar dissipation rate distribution. Results in (b) are at a time 20 ms later than those in (a).

CO_2, OH, and NO have been given by Barlow et al. [16,17]. Comparison of the predicted results with the experimental data has been presented and discussed further in Ref. [18]. In general, the agreement of predictions and experimental data is considered very good.

Unconditionally Filtered Scalar Dissipation Rate

Spatial $\tilde{\chi}$-distribution

Figure 1 shows instantaneous distributions of the unconditionally filtered scalar dissipation rate, $\tilde{\chi}$, obtained from equation 5. Figure 1b shows a realization at a time approximately 20 ms later than that in 1a. The figures are presented at the same point in time as the temperature distributions given in Ref. [18]. The stoichiometric contour, which indicates the approximate location of the reaction zone, is also indicated. Regions of high scalar dissipation rate appear in layerlike structures, which are directed inward. In general, these layers are well aligned with the stoichiometric contour, when this is directed inward. Since both the stoichiometric contour and the high scalar dissipation rate layers cannot be inclined to the mean flow over a long distance, the stoichiometric contour diverges outward again to the next surrounding dissipation layer. This usually occurs at much higher angles relative to the axis of the jet. Since the inwardly directed stoichiometric contours appear at high scalar dissipation rate, the corresponding temperature distribution is very narrow, as corroborated by Ref. [18]. In contrast, the outwardly directed contours are associated with broad temperature regions.

Similar behavior has been observed by Feikema et al. [26] in measurements of the scalar dissipation rate in a non-reacting turbulent jet. They found that the scalar dissipation rate appears in layers, which are inclined at approximately 45° to the flow. Rehm and Clemens [27,28] found that the minimum compressive strain in turbulent jet flames appears in similar layers, which are also inclined at 45° to the flow and aligned with the reaction zone. Rehm and Clemens [28] have also shown from experiments in non-reacting jets that the minimum compressive strain layers are well aligned with the scalar dissipation rate layers. In experiments of reactive jets,

they also observed the broadening of the reaction zone in instances where this is directed away from the jet axis. All these findings are consistent with the current simulation. However, on average the inclination angle of the dissipation layers in Fig. 1 seems to be smaller than 45° to the direction of the flow.

Single-point time records of $\tilde{Z}$ and $\tilde{\chi}$

Single-point time records of the mixture fraction and the scalar dissipation rate at the centerline position at $x/D = 30$ are given in Fig. 2. As shown in Fig. 2 and also by Pitts et al. [1] for non-reacting jet experiments, the scalar dissipation rate fluctuates at a much higher frequency than the mixture fraction. Also, the mean duration of a peak at high scalar dissipation rate appears to be much longer than a peak at low scalar dissipation rate. Donbar et al. [10] found that for a turbulent jet flame with a Reynolds number $Re = 18{,}600$, which is very similar to the present case, that the strain rate fluctuates at approximately 10 kHz. The frequency of the scalar dissipation rate fluctuations at $x/D = 30$ shown in Fig. 2 can be estimated to be 2.5 kHz. This frequency however, varies strongly with the nozzle distance.

It should be noted here that even the shortest fluctuations appearing in Fig. 2 are well resolved in time, such that the time-step of the calculation does not impose any filtering. The frequency that can be resolved by the computational mesh might be estimated by the average cell size in the axial direction and the time averaged axial velocity as $f_{\mathrm{Res}} \approx 10$ kHz. Since it has been found in the reacting jet experiments of Donbar et al. [10] and also in simulations of counterflow diffusion flames by Saitoh and Otsuka [9] that the flame chemistry does not respond to fluctuations in the strain rate higher than 10 kHz, it appears that the spatial filtering is not restrictive for the use of the predicted scalar dissipation rate in chemistry calculations.

Figure 2 also reveals one other very important mixing aspect which is not directly related to the scalar dissipation, but should still be discussed here. Pitts et al. [1] have investigated large-scale turbulent structures in a non-reacting jet. As one of the most important proofs of the formation of these structures, they discuss the observation of ramplike structures in one-point time records of scalars in turbulent jets. These ramplike structures can also be observed in the resolved mixture fraction record shown in Fig. 2. In general, the increase of the mixture fraction occurs much more rapidly than the following decrease. This seems to corroborate that the current simulations are capable of describing large-scale mixing phenomena, which are believed to be very important for the overall structure and development of the scalar field.

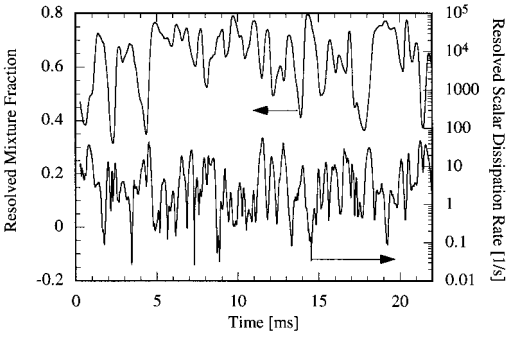

FIG. 2. Time records of the resolved mixture fraction and the scalar dissipation rate on the centerline at $x/D = 30$.

The pdf of $\tilde{\chi}$

The pdf of the scalar dissipation rate has been investigated in many studies [1,29,30]. It has been found that the distribution of χ is log-normal. In terms of the density-weighted filtered quantities, this can be expressed as

$$\tilde{P}(\tilde{\chi}) = \frac{1}{\tilde{\chi}\sqrt{2\pi}} \exp\left(-\frac{(ln\tilde{\chi} - \mu)^2}{2\sigma^2}\right) \qquad (9)$$

Here, μ and σ are parameters of the pdf, which essentially represent the mean and the fluctuation about the mean, respectively. From non-reacting jet experiments, Effelsberg and Peters [29] have found the parameter σ to have a value close to unity. The evaluation of the pdf of $\tilde{\chi}_{\mathrm{st}}$ using all computational cells in the particular cross-section is presented in Fig. 3 for $x/D = 15$ and $x/D = 30$. Also shown is the pdf evaluated from equation 9 with $\sigma = 1$ and the appropriate values for μ to match the mean scalar dissipation rate, viz. $\mu = 4.7$ and 3.2 for $x/D = 15$ and 30, respectively. The comparison shows that

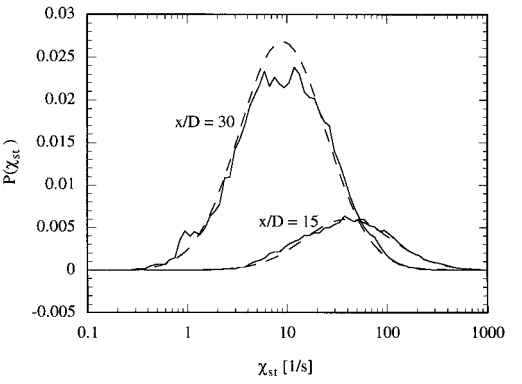

FIG. 3. The pdf of the stoichiometric resolved scalar dissipation rate at $x/D = 15$ and $x/D = 30$ (solid lines) compared to log-normal pdfs (dashed lines), with $\sigma = 1$ from equation 9.

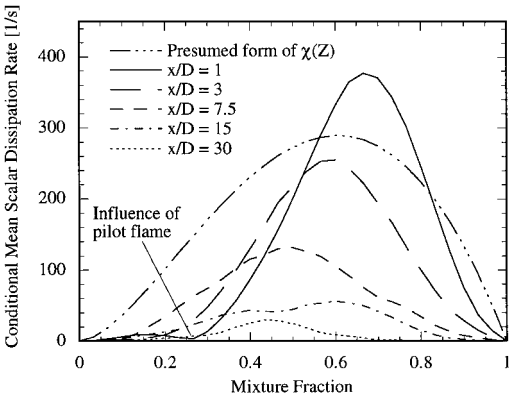

FIG. 4. Conditional scalar dissipation rate at different downstream locations. Also shown is a commonly presumed form of the mixture fraction dependence of the scalar dissipation rate.

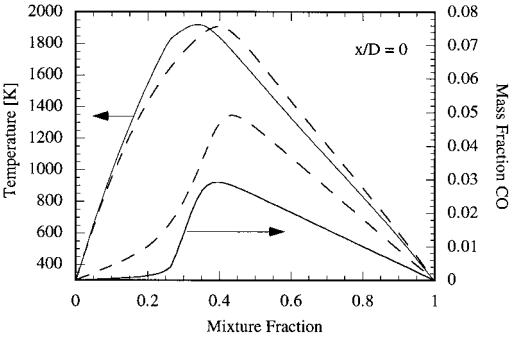

FIG. 5. Influence of the mixture fraction dependence of the scalar dissipation rate on the flamelet solution at the nozzle exit. Calculation using $\chi(Z)$ from equation 8 (solid lines) compared to solution with $\chi(Z)$ (dashed lines) presumed according to Ref. [14].

the distribution of $\tilde{\chi}_{st}$ at both positions is almost perfectly log-normal, and also that $\sigma = 1$ seems to be a very good approximation for the case investigated. The same value of σ is observed at $x/D = 45$.

Conditional Mean Scalar Dissipation Rate

Results for the conditional mean scalar dissipation rate at different downstream locations determined from equation 8 are shown in Fig. 4. The comparison with a presumed shape of $\chi(Z)$ from Ref. [14] indicates that this simple function is not applicable in the present case. Within the pilot stream, which is at $Z = 0.27$, the scalar gradient, and hence the scalar dissipation rate, is zero. Even at far downstream locations, the shape of the scalar dissipation rate is still influenced by the pilot flame.

The computed shape at $x/D = 1$ provides an interesting explanation of the stabilizing effect of a pilot flame. The pilot causes the scalar dissipation rate to be zero at the pilot mixture fraction, which in turn also causes the scalar dissipation rate at stoichiometric mixture fraction ($Z_{st} = 0.35$) to be small. However, by interdiffusion with the surrounding mixing layer this value strongly increases with downstream direction. Also, the same diffusive effect causes the scalar dissipation rate generally to decrease strongly with downstream direction [31]. Hence, in the present case, χ_{st} first increases until approximately $x/D = 7.5$, and then decreases. If the maximum value stays smaller than the extinction limit, $\chi_{st,q}$, the flame stabilizes at the pilot. However, if it exceeds $\chi_{st,q}$, the flame will exhibit local extinction or even blow off. This also explains why it is favorable to have the pilot mixture fraction close to the stoichiometric mixture fraction, which keeps χ_{st} lower, and also to have a broad pilot flow, because then the increase of χ around the pilot will be much slower.

The influence of the scalar dissipation rate model on the initial conditions for the unsteady flamelet calculation, which is assumed to be the steady flamelet solution with $\chi(Z)$ evaluated from equation 8 at $x/D = 0$, is given in Fig. 5. The flamelet solution for the temperature and the CO mass fraction are compared to the solution using the presumed $\chi(Z)$ of Ref. [14]. Because of the influence of the pilot, the flame is substantially shifted to the lean side. Also, as shown in Fig. 4, the presumed function overestimates the scalar dissipation in the lean part of the flame, leading to a substantial overprediction of the CO mass fraction.

Influence of Resolved Scalar Dissipation Rate Fluctuations

The influence of the scalar dissipation rate fluctuations, which are resolved by equation 8, are investigated next. As mentioned above, the pdf of the unconditional scalar dissipation rate clearly reveals a log-normal shape with $\sigma = 1$. Because the conditional scalar dissipation rate given by equation 8 is a spatial conditional average, which has for the present study and for the results presented in Ref. [18] been performed over all computational cells in cross sections normal to the jet axis, the pdf of $\langle\chi|Z\rangle$ is much narrower than the pdfs shown in Fig. 3. This, however, can be substantially improved by sampling over smaller areas. In order to analyze the influence of the resolved fluctuations on the flame structure, 250 different instantaneous scalar dissipation rate and mixture fraction fields were recorded from the calculations presented in Ref. [14]. These calculations were performed using the time-averaged scalar dissipation rate. Using these data, 250 unsteady flamelet calculations were performed, and the resolved

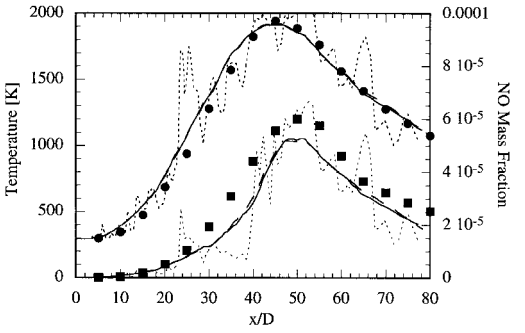

FIG. 6. Ensemble-averaged temperature and NO mass fraction determined as the average over multiple instantaneous realizations (solid lines) compared to a calculation using a time average of the scalar dissipation rate (dashed lines). Also given is an example for one instantaneous realization (dotted line).

temperature and mass fractions were evaluated using equation 2. The results were ensemble averaged, and the temperature and the NO mass fraction of these calculations are compared along the centerline to the calculations using the time average of the scalar dissipation rate and the experimental data given by Barlow et al. [16,17] in Fig. 6. Also given in Fig. 6 is one example of an instantaneous solution of temperature and NO mass fraction. This solution shows temperature fluctuations, which can be of the order of 700 K. However, almost no differences in the results of both methods can be observed, indicating that the resolved fluctuations of the scalar dissipation rate influence the flame structure only very weakly, and also that the strong fluctuations in the instantaneous solution given in Fig. 6 are essentially caused by fluctuations in the resolved mixture fraction and its subgrid scale variance. Both methods yield good agreement with the experimental data for the present case. However, if local extinction events start to become important, the pdf of the scalar dissipation rate has to be determined much more accurately, and averages over complete cross sections can no longer be used.

Conclusions

The present study provides a discussion of scalar mixing and the scalar dissipation rate in large-eddy simulations. The results from an LES of the Sandia flame D have been used to compare the predictions of the mixture fraction field and the scalar dissipation rate with mostly qualitative experimental data. In agreement with experimental data, it has been found that regions of high scalar dissipation rate are organized in layerlike structures that are inwardly inclined to the mean flow and aligned with the reaction zone.

The fluctuation frequency of the scalar dissipation rate has been discussed in the context of the spatial and temporal resolution of the current simulation, and the findings are that the resolution used in the present investigation is not restrictive for the predictions of the scalar dissipation rate. Single-point time records of the mixture fraction have been found to reveal ramplike structures, which are also evident in experimental data for non-reacting jets. Pitts et al. [1] regarded this as one of the most important proofs for the occurrence of large-scale turbulent structures in turbulent jets.

The pdf of the stoichiometric scalar dissipation rate was found to be described accurately by a log-normal pdf with a value of $\sigma = 1$. The ratio of the integral time scales of scalar and velocity fluctuations, which is commonly used in Reynolds-averaged turbulence models to determine the unconditionally averaged scalar dissipation rate, was evaluated using the resolved velocity and scalar field.

A model for the conditional scalar dissipation rate has been suggested that accounts for the influence of local deviations from a simple mixing layer structure. Furthermore, this model has been demonstrated to account for the strong influence of a pilot in the near-field of a turbulent jet flame.

Finally, the influence of the fluctuations resolved by the model for the conditional scalar dissipation rate on the flame structure was investigated by comparing averages over simulations using instantaneous scalar dissipation rate histories with a simulation using the time-averaged scalar dissipation rate. The results for temperature and NO mass fraction are not influenced by the scalar dissipation rate fluctuations. However, the model would need to be refined for instances in which local extinction events become important.

Acknowledgments

Support by the U.S. Department of Energy within the ASCI program is acknowledged. The authors also thank George Kosály for many helpful discussions.

REFERENCES

1. Pitts, W. M., Richards, C. D., and Levenson, M. S., *Large- and Small-Scale Structures and Their Interactions in an Axisymmetric Jet,* NIST internal report NISTIR 6393, National Institute of Standards and Technology, Gaithersburg, MD, 1999.
2. Spalding, D. B., *Proc. Combust. Inst.* 13:649–657 (1971).
3. Bilger, R. W., *Combust. Sci. Technol.* 110:155–170 (1976).
4. Peters, N., *Prog. Energy Combust. Sci.* 10:319–339 (1984).
5. Peters, N., *Proc. Combust. Inst.* 21:1231–1250 (1986).

6. Pope, S. B., *Prog. Energy Combust. Sci.* 11:119–192 (1985).
7. O'Brien, E. E., in *Turbulent Reacting Flows,* (P. A. Libby and F. A. Williams, eds.), Springer, 1980, p. 185.
8. Klimenko, A. Y., and Bilger, R. W., *Prog. Energy Combust. Sci.* 25:595–687 (1999).
9. Saitoh, T., and Otsuka, Y., *Combust. Sci. Technol.* 12:135–146 (1976).
10. Donbar, J. M., Driscoll, J. F., and Carter, D. C., *Combust. Flame,* in press (2000).
11. Barlow, R. S., and Chen, J.-C., *Proc. Combust. Inst.* 24:231–237 (1992).
12. Haworth, D. C., Drake, M. C., Pope, S. B., and Blint, R. J., *Proc. Combust. Inst.* 24:589–597 (1988).
13. Mauss, F., Keller, D., and Peters, N., *Proc. Combust. Inst.* 25:693–698 (1990).
14. Pitsch, H., Chen, M., and Peters, N., *Proc. Combust. Inst.* 27:1057–1064 (1998).
15. Pitsch, H., *Combust. Flame,* in press, (1999).
16. Barlow, R. S., and Frank, J. H., *Proc. Combust. Inst.* 27:1087–1095 (1998).
17. www.ca.sandia.gov/tdf/Workshop.html, Sandia National Laboratory, 1998 (updated June 7, 2000).
18. Pitsch, H., and Steiner, H., unpublished work (1999).
19. Pierce, C. D., and Moin, P., *Phys. Fluids A* 10:3041–3044 (1998).
20. Moin, P., Squires, K., Cabot, W., and Lee, S., *Phys. Fluids A* 3:2746–2757 (1991).
21. Girimaji, S. S., and Zhou, Y., *Phys. Fluids A* 8:1224–1236 (1996).
22. Kim, J. S., and Williams, F. A., *SIAM J. Appl. Math.* 53:1551–1566 (1993).
23. Bushe, W. K., and Steiner, H., *Phys. Fluids A* 11:1896–1906 (1999).
24. Janicka, J., and Peters, N., *Proc. Combust. Inst.* 19:367–374 (1982).
25. Hassel, E., www.ca.sandia.gov/tdf/Workshop.html, Sandia National Laboratory, 1998 (updated June 7, 2000).
26. Feikema, D. A., Everest, D., and Driscoll, J. F., *AIAA J.* 34:2531–2538 (1996).
27. Rehm, J. E., and Clemens, N. T., *Proc. Combust. Inst.* 27:1113–1120 (1998).
28. Rehm, J. E., and Clemens, N. T., "The Association of Scalar Dissipation Rate Layers and OH Zones with Strain, Vorticity, and 2-D Dilatation Fields in Turbulent Nonpremixed Jets and Jet Flames," AIAA paper 99-0676, Thirty-Seventh AIAA Aerospace Sciences Meeting and Exhibit, Reno, NV, Jan. 11–14, 1999.
29. Effelsberg, E., and Peters, N., *Proc. Combust. Inst.* 22:693–700 (1988).
30. Dahm, W. J. A., and Buch, K. A., *Phys. Fluids A* 1:1290–1293 (1989).
31. Peters, N., and Williams, F. A., *AIAA J.* 21:423–429 (1983).

COMMENTS

William Mell, University of Utah, USA.

1. Did you also implement a quasi-steady version of the flamelet model? If so, how did it perform compared to your transient model?
2. What boundary conditions did you use for the laminar flamelet model? In particular, were transient effects important?
3. Did you consider regimes in which buoyancy played a greater role (rather than momentum) in the flow? It seems likely that in such a situation the axial velocity (which gives the Lagrangian time) may not be as representative of the flamelets at a given axial position.

Author's Reply.

1. Predictions using a quasi-steady model have been shown to be more accurate if radiation is neglected. For the investigated configuration, the application of the quasi-steady model leads thereby to an overprediction of the temperature. This leads to an overprediction of the NO mass fraction by approximately a factor of 2. However, for the conclusions of the present paper regarding the scalar mixing process, the use of a quasi-steady model will show hardly any influence.
2. Using the models proposed in the present paper, the predicted conditional scalar dissipation rate becomes small if the pdf of the mixture fraction goes to zero. This can be seen in Fig. 4. In the region of zero scalar dissipation rates, the diffusion term in the flamelet equation is zero. This implies that the boundary conditions of the flamelet solution are homogeneous reactor solutions at an effective maximum mixture fraction.
3. We did not consider a configuration where buoyancy is important. However, the Lagrangian time can still be determined from the axial velocity, which would change accordingly if the momentum flux were dominated by buoyancy.

•

A. Y. Klimeuto, The University of Queensland, Australia. I am certain that the topic of the presentation, investigation into the influence of fluctuations of the conserved scalar-dissipation on combustion, is most important for flamelet modeling. However, I think that one question needs some clarification. The subgrid model used by the authors ignores the subgrid fluctuations which can be expected to be most significant for the scalar dissipation. Can this factor affect the conclusions of the present work?

Author's Reply. In the present model, the subgrid part of the scalar dissipation rate is considered by the use of a subgrid model. Because of the subgrid filtering, the pdf

of the scalar dissipation rate and also the frequency of its fluctuations might be influenced. It is shown in Fig. 3 that the resolved pdf is in good agreement with experimental findings. This suggests that the filtering only influences the tails of the pdf. It is also mentioned in the paper that the present simulation can resolve a frequency of 10 kHz. It has been shown in experiments (Ref. [10] in this paper) and simulations of counterflow diffusion flames (Ref. [9] in this paper) that the flame chemistry does not respond to higher frequencies.

•

Andrew Pollard, Queen's University, Canada. Can you confirm that the scalar dissipation is coincident with regions of high axial vorticity (i.e., braids between azimuthal vortex rings)?

Author's Reply. Obviously, the regions of high scalar dissipation rate are located between large-scale azimuthal vortical structures. However, from the observations we made in this study there is not clear evidence that these structures appear in rings, which would be connected by secondary axial vortices. This might still be the case, but we have not looked explicitly into these details.